Barrierless evolution of structure during the submillisecond refolding reaction of a small protein

Kalyan K. Sinha and Jayant B. Udgaonkar*

National Centre for Biological Sciences, Tata Institute of Fundamental Research, Bangalore 560065, India

Communicated by Robert L. Baldwin, Stanford University, Stanford, CA, April 2, 2008 (received for review January 2, 2008)

To determine whether a protein folding reaction can occur in the absence of a dominant barrier is crucial for understanding its complexity. Here direct ultrafast kinetic measurements have been used to study the initial submillisecond (sub-ms) folding reaction of the small protein barstar. The cooperativity of the initial folding reaction has been explored by using two probes: fluorescence resonance energy transfer, through which the contraction of two intramolecular distances is measured, and the binding of 8-anilino-1-naphthalene sulfonic acid, through which the formation of hydrophobic clusters is monitored. A fast chain contraction is shown to precede the formation of hydrophobic clusters, indicating that the sub-ms folding reaction is not cooperative. The observed rate constant of the sub-ms folding reaction monitored by 8-anilino-1-naphthalene sulfonic acid fluorescence has been found to be the same in stabilizing conditions (low urea concentrations), in which specific structure is formed, and in marginally stabilizing conditions (higher urea concentrations), where virtually no structure is formed in the product of the sub-ms folding reaction. The observation that the folding rate is independent of the folding conditions suggests that the initial folding reaction occurs in the absence of a dominant free energy barrier. These results provide kinetic evidence that the formation of specific structure need not be slowed down by any significant free energy barrier during the course of a very fast protein folding reaction.

noncooperative | submillisecond protein folding

The nature of the energy barriers that slow down protein folding reactions is poorly understood (1–3). There is no theoretical basis to the common assumption that any elementary step of a protein folding reaction should have only a single dominant free energy barrier instead of many distributed smaller barriers (4). There is only an empirical basis to the application of transition state (TS) theory to protein folding reactions, which posits that a dominant barrier ($>3\ k_BT$) slows down the folding reaction. Yet the complex folding reactions of proteins appear to be described remarkably well by TS theory. On the other hand, the alternative hypothesis, that folding is gradual and barrierless, occurring as a diffusive process that encounters distributed barriers only about k_BT in energy (2, 5), is difficult to validate experimentally. The defining feature of a barrier-limited, cooperative transition is the coexistence of only two structural forms separated by the activation barrier, and the kinetics of such an all-or-none transition are defined by waiting times, with the actual passage times being too fast to observe. In contrast, only one species changes structure and free energy during a barrierless, gradual transition, making such a continuous transition potentially amenable to continuous observation in real time. To distinguish an all-or-none folding transition from a gradual transition remains, however, a difficult challenge (6, 7).

Recent steady-state (8, 9) and single-molecule FRET studies (10, 11), carried out under equilibrium conditions, have indicated that the transition between the unfolded and collapsed forms during the folding of several proteins may be so highly noncooperative as to be a gradual structural transition. Several other equilibrium unfolding studies using high-resolution structural probes have also provided evidence for gradual structural changes during unfolding (12–15). Such gradual structural changes may involve the crossing of many small free energy barriers rather than only one dominant barrier. But definitive kinetic evidence for a protein folding reaction occurring in the absence of a dominant free energy barrier has been scarce.

Most proteins fold with exponential kinetics, and nonexponential folding kinetics have been observed only in specific folding conditions for very few proteins (3, 16, 17). Barrier-limited processes display exponential kinetics, but so may barrierless processes (16, 17). Indeed, a barrierless chemical reaction will display exponential kinetics if its product ends up occupying a harmonic potential well (18), and, in the context of protein folding, a diffusive process may have kinetics very similar to exponential kinetics (19–21). Barrierless processes may also display nonexponential kinetics (3, 16), but nonexponential kinetics can also arise because of multiple folding pathways (22, 23). Obviously a barrierless reaction cannot be distinguished from a barrier-limited one solely on the basis of the folding kinetics being exponential or nonexponential (19–21). For a few proteins, barrierless or downhill folding has been identified from the observed tuning of the folding kinetics by a change in solvent or temperature, or by mutation: the kinetics were observed to switch smoothly from single exponential to complex (probe-dependent, multiexponential, or nonexponential) as folding conditions are made more native-like (3, 16, 21).

In the present study, the degree of cooperativity in the initial, submillisecond (sub-ms) folding reaction of the small protein barstar has been delineated by using multiple structural probes in ultrafast kinetic studies. Much is known about the folding mechanism of barstar (24–30), and earlier studies with millisecond time resolution had indicated, albeit indirectly, that the initial, sub-ms folding reaction of barstar is a gradual process (8, 9). A very early collapsed structure-less globule, U_C, gets transformed into a structured early intermediate, I_E (9, 25, 26), at a few milliseconds of folding. I_E then transforms to a late intermediate and native protein in the subsequent major folding reaction in the 100-ms time domain (24, 25). Here the formation of I_E has been monitored by using two probes, FRET as a probe for chain contraction and the fluorescence of protein-bound 8-anilino-1-naphthalene sulfonic acid (ANS) as a probe for hydrophobic clustering. An ultrafast chain collapse process is shown to precede a very fast hydrophobic clustering reaction. It is further demonstrated that the sub-ms folding reaction does not involve the crossing of a dominant free energy barrier, even though it results in the formation of specific structure.

Results and Discussion

Specific Structure Is Present in the Product of the Sub-ms Folding Reaction. Two single Cys-containing, single Trp-containing mutant forms of barstar, Cys40 and Cys82, were used in this study.

Author contributions: K.K.S. and J.B.U. designed research; K.K.S. performed research; and K.K.S. and J.B.U. wrote the paper.

The authors declare no conflict of interest.

*To whom correspondence should be addressed. E-mail: jayant@ncbs.res.in.

This article contains supporting information online at www.pnas.org/cgi/content/full/0803193105/DCSupplemental.

The folding kinetics of these mutant variants are similar to those of wild-type barstar and other similar mutant variants (9, 12). Here, folding was studied in strongly stabilizing (0.25 M urea) to marginally stabilizing (≈1.5 M urea) conditions.

To show that significant structure does indeed develop during the sub-ms folding reaction, the refolding kinetics of Cys40 were studied first with ms time resolution using far-UV CD (Fig. 1*a*) and ANS binding (Fig. 1*b*) as probes. The extent of spectroscopic change that occurs in the unobservable burst phase of the millisecond stopped-flow kinetic measurements represents the extent of structure formation that occurs in the initial sub-ms folding reactions. Fig. 1 *a* and *b* shows that a substantial increase in far-UV CD, as well as ANS fluorescence consequent to binding, occurs in the unobservable burst phase for folding in strongly stabilizing conditions. The former indicates an increase in helical secondary structure, and the latter indicates an increase in hydrophobic clustering that is absent in the unfolded (U) and folded (N) proteins (24). Thus, the product of sub-ms folding possesses specific secondary structure and hydrophobic clusters. Both types of structure in this sub-ms folding product disappear in a nonsigmoidal but synchronous manner when its stability is reduced by increasing the urea concentration in which folding is carried out (Fig. 1*c*).

Submillisecond Folding of Barstar Is Not All-or-None. A continuous-flow microsecond mixer was constructed to study the first 1 ms of the folding of barstar [supporting information (SI) Fig. S1]. When folding was carried out in 0.8 M urea, hydrophobic clustering, as represented by the accompanying increase in ANS binding and fluorescence, was seen to increase exponentially with an apparent rate constant of 4,320 ± 440 s^{-1} (Fig. 2*a*). The very fast phase observed here continues into a fast millisecond exponential decay phase as the folding reaction progresses, which is monitored on a stopped-flow mixer.

To test whether the dimensions of the polypeptide chain contract simultaneously with the formation of hydrophobic clusters, the sub-ms contraction of two intramolecular distances, one separating Trp53 and Cys40 in the Cys40TNB protein and another separating Trp53 and Cys82 in the Cys82TNB protein, was measured by FRET in 0.8 M urea (Fig. 2 *b* and *c*). Trp53 was the donor for both of the FRET pairs (8, 9, 12), whereas the acceptor TNB group was attached to a Cys residue placed at position 40 in Cys40TNB and at position 82 in Cys82TNB. Earlier studies had shown that the stabilities and folding kinetics of the labeled and unlabeled mutant variants were similar (9, 12). FRET was measured by monitoring the fluorescence of the labeled proteins at 380 nm. The decrease in the fluorescence at 380 nm is directly proportional to the increase in FRET efficiency, as described earlier (8, 9). For both intramolecular distances, the major phase of the FRET-monitored kinetics appears to be complete in the first 250 μs of the folding reaction, suggesting that the overall dimensions of the polypeptide chain have contracted at this time. Because the apparent rate of this ultrafast phase is >10,000 s^{-1}, only the last 20% of the total amplitude of FRET change could be resolved. Hence, there is some uncertainty in the determination of the exact values of the rate constants, even though the signal-to-noise ratio in the observed ultrafast change is good. In the case of Cys40TNB, the data are well described by a single exponential and extrapolate to a value at $t = 0$ that is much lower than the signal of the unfolded protein in 8 M urea (Fig. 2*b*). This observation suggests that the ultrafast contraction of the Trp53-Cys40TNB distance might involve more than one kinetic phase with the faster phase being unobservable with the current dead time of the continuous-flow mixer. On the other hand, in the case of Cys82TNB, the data are best fit to a sum of two exponentials, and the fit extrapolates at $t = 0$ to the signal of the unfolded protein in 8 M urea (Fig. 2*c*). The ultrafast contraction of the Trp53-Cys82TNB distance can therefore be fully resolved but still occurs in two kinetic phases. The observation of a difference in the kinetics

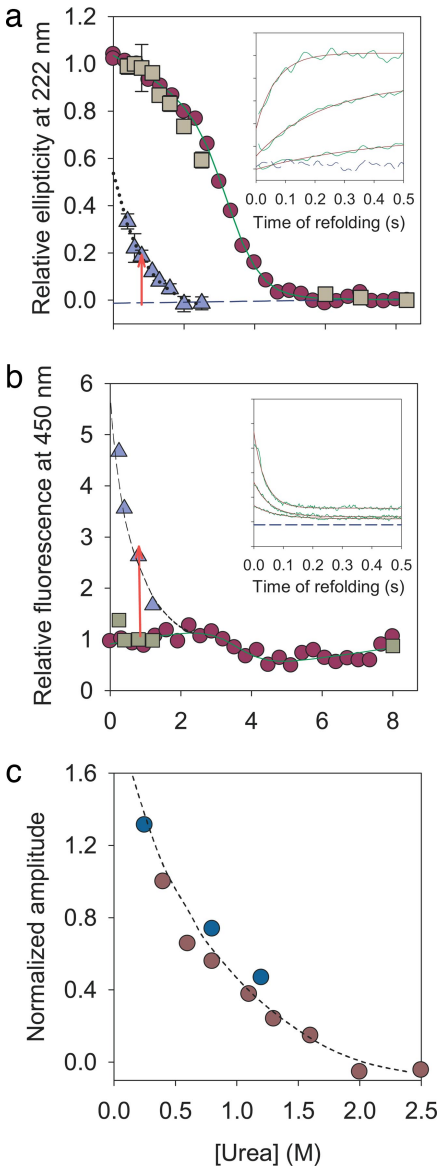

Fig. 1. Structure is present in the product of the sub-ms folding reaction. Shown here are the kinetic amplitudes of the ms refolding reaction of barstar monitored by different probes: far-UV CD (*a*) and ANS fluorescence (*b*). In each of the panels, the square represents the kinetic $t = \infty$ signal, and the triangles represent the $t = 0$ signal obtained by fitting the kinetic traces obtained in the >1-ms time domain to an exponential equation. The equilibrium amplitudes are shown as circles. In each of the panels, the solid line through the equilibrium unfolding data is a fit to a two-state N⇌U model, and the dashed line is the extrapolated unfolded protein baseline. The arrow represents the change in signal that occurs in the sub-ms time domain for folding in 0.8 M urea. In each panel, the dotted line through the $t = 0$ data points has been drawn by inspection only. In *a* all of the data points have been normalized to a value of 1 for the signal of native protein in 0.6 M urea. The *Inset* in *a* shows representative kinetic traces of the far-UV CD-monitored refolding reactions in 0.4 M (bottom trace), 1.6 M (middle trace), and 2.5 M (top trace) urea concentrations. In *b* all of the data points have been normalized to a value of 1 for the $t = \infty$ signal of refolding in 0.8 M urea. The *Inset* in *b* shows representative kinetic traces of the ANS-fluorescence-monitored kinetics in 0.25 M, 0.8 M, and 1.2 M urea. (*c*) A comparison of the burst phase amplitudes observed in the far-UV CD-monitored millisecond kinetic experiment (brown circles) to the total amplitude of the ANS-fluorescence-monitored refolding kinetic experiment (blue circles). The data have been normalized to a value of 1 for the value of the amplitude observed in 0.4 M urea. The dashed line through the data has been drawn by inspection only. Where shown, error bars indicate the spreads in the values determined from two or more repetitions of the experiments.

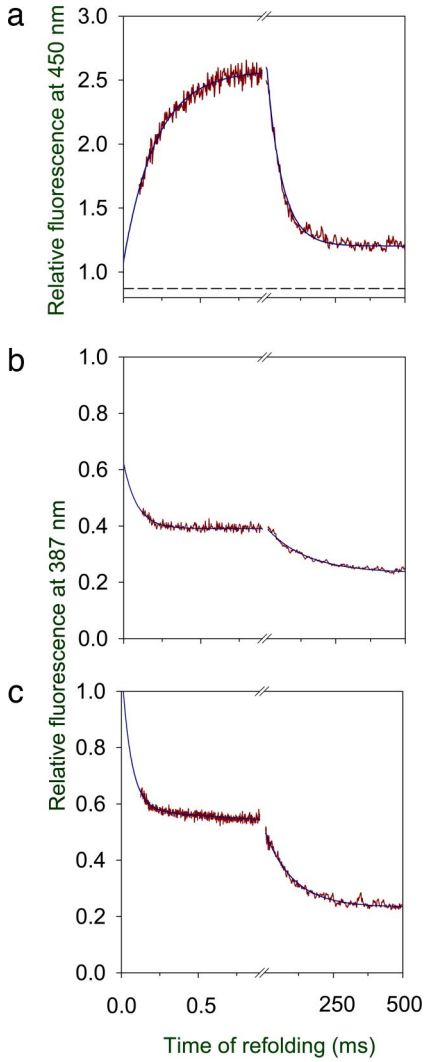

Fig. 2. Sub-ms refolding kinetics. The kinetics of refolding in 0.8 M urea were monitored by ANS fluorescence (*a*) and FRET (*b* and *c*). In all of the panels, the sub-ms data from the continuous-flow mixer are normalized to the millisecond data from stopped-flow mixing for comparison. (*a*) The kinetics monitored by ANS fluorescence fit to a single exponential with a rate constant of 4,320 s^{-1}. The data in *a* are normalized to a value of 1 for the $t = \infty$ signal of the millisecond refolding trace in 0.8 M urea. The dashed line represents the signal of the unfolded protein in 8 M urea. The kinetics of contraction of two intramolecular distances Trp53-Cys40TNB and Trp53-Cys82TNB are shown in *b* and *c*, respectively. The line through the data is a fit to an exponential equation. For Cys40TNB, the rate constants obtained from the fit are 11,500 s^{-1} and 7 s^{-1} for the ultrafast sub-ms phase and the fast millisecond phase, respectively. For Cys82TNB, the sub-ms phase data fit to a biexponential equation with rate constants of 16,300 and 490 s^{-1}; the rate constant of the fast millisecond phase is 10 s^{-1}. In *b* and *c* the data are normalized to a value of 1 for the unfolded protein signal in 8 M urea.

of contraction of the two intramolecular distances is in agreement with the results of earlier millisecond kinetic measurements, which had indicated that the contraction of different intramolecular distances during the sub-ms folding reaction is not synchronized across different regions of the protein molecule (8, 9).

The difference in the rates of the sub-ms folding reaction monitored by FRET and by ANS fluorescence suggests that an ultrafast chain contraction precedes the very fast clustering of hydrophobic residues in the folding polypeptide chain. This could happen possibly because collapse is promoted by the formation of intrapeptide hydrogen bonds, which are favored over peptide–water hydrogen bonds, in folding conditions (31), or because of a change in ϕ–ψ backbone preferences with a change in the solvent conditions (32). Irrespective of its origin, the ultrafast chain contraction is significant because it brings sequence-distal hydrophobic residues into proximity; i.e., it may guide and facilitate the formation of hydrophobic clusters.

Absence of a Significant Free Energy Barrier During the Sub-ms Folding Reaction. Because the sub-ms folding reaction is well separated in time from subsequent folding reactions that occur in the 100-ms time domain (Fig. 1 *a Inset* and *b Inset*), the observed FRET-measured ultrafast rate as well as the ANS-fluorescence-measured very fast rate represent the rates of events leading to the formation of the early intermediate I_E identified previously on the folding pathway of barstar (25, 26). In the previous studies, I_E was found to be fully populated at a few milliseconds of folding, and the ANS-fluorescence-measured rate is likely to be the direct rate of formation of I_E. The multistep nature of the sub-ms folding reaction observed here implies that the U-to-I_E reaction is not all-or-none. To test whether any significant free energy barrier exists between U and I_E, the sub-ms refolding kinetics were studied in different folding conditions, which would confer different degrees of stability to N and I_E, as well as to any TS, if present (25).

The rate constant of a protein folding reaction in solution has the form

$$k = \frac{c}{\eta} e^{-\frac{G^{\ddagger}}{RT}},$$

where c is a constant, η is the solvent viscosity, $\Delta G^{\ddagger}$ is the free energy of activation, R is the universal gas constant, and T is the reaction temperature. The exponential term slows down the folding reaction from its diffusion-controlled speed limit. In the absence of an activation barrier, the exponential term disappears and the folding reaction can proceed at its speed limit. If an activation barrier is present, it can be modulated by changing $\Delta G^{\ddagger}$. Because $\Delta G^{\ddagger}$ would have a linear dependence on denaturant concentration, k would be expected to have a significant exponential dependence on denaturant concentration for a barrier-limited process, and it should be independent of denaturant concentration if no significant free energy barrier is present (6).

The very fast rate of formation of I_E is indeed observed to be independent of urea concentration (Fig. 3 *a* and *b*), indicating that the polypeptide chain does not encounter a sizeable free energy barrier while folding to I_E. This interpretation gains credence from several earlier observations: (*i*) the structure of I_E is different in the presence of different osmolytes and different salts (25, 26); (*ii*) different intramolecular distances in I_E contract in a gradual and asynchronous manner, upon a reduction in denaturant concentration (9); (*iii*) the free energy difference between U and I_E turns out to be less than k_BT (25, 26) if the U-to-I_E transition is assumed to be barrier-limited; (*iv*) I_E is loosely packed throughout its structure (33) and hence is expected to form with a lack of cooperativity (20, 34); and (*v*) most importantly, gradual structural changes in the folded as well as unfolded forms of barstar have been detected in equilibrium unfolding studies (12, 13).

The magnitude of the exponential term in the expression for the rate constant k can also be altered by changing T. Fig. 3*c* shows that the very fast rate of formation of I_E has a very weak dependence on temperature. The observed dependence is less than the expected temperature dependence of η, which is known to increase exponentially with an increase in $1/T$ (35). Hence, if the temperature dependence of viscosity is taken into account, the activation enthalpy for the very fast folding reaction turns out to be negative, which is taken as a signature for a folding reaction

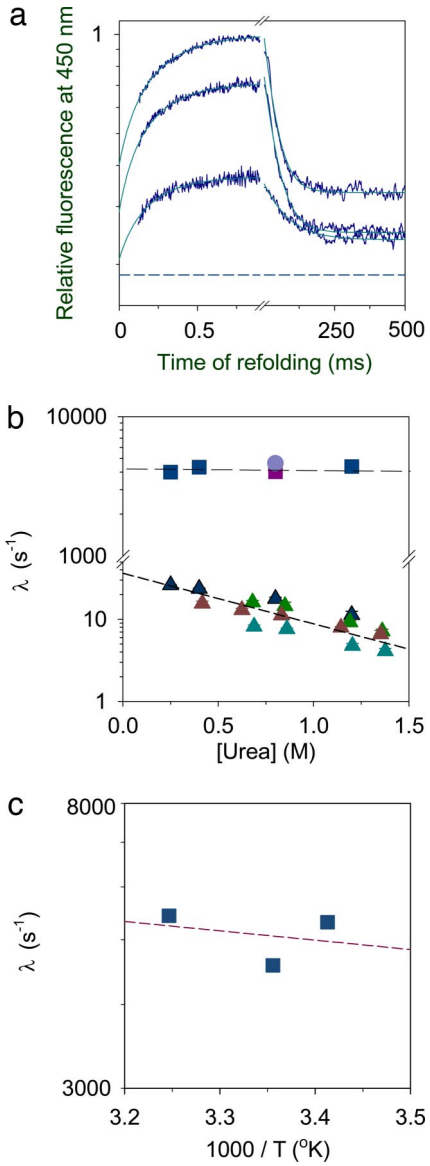

Fig. 3. Dependence of the folding kinetics on urea concentration. (*a*) Representative very fast kinetic traces in final urea concentrations of 0.25 M (top trace), 0.4 M (middle trace), and 1.2 M (bottom trace) are shown. The very fast phase corresponding to the sub-ms exponential rise of the ANS fluorescence was captured by using the microsecond mixer. The >1-ms part of the data was obtained by using a stopped-flow mixer under identical conditions. The dashed line represents the unfolded protein baseline. The *y* axis is shown on a log scale for a comparison of the kinetics in different urea concentrations. The data shown here are normalized to a value of 1 for the $t = \infty$ signal of the sub-ms kinetic refolding trace obtained in 0.25 M urea. The lines through the data are fits to a two-exponential equation. (*b*) Comparison of the kinetics monitored by different probes. Shown are the very fast rate constants of the sub-ms folding reaction (blue squares) and the fast rate constants (blue triangles) of the stopped-flow-monitored millisecond folding reaction, both obtained from the measurement of the ANS-fluorescence-monitored refolding kinetics; the very fast rate constant of the ANS-fluorescence-monitored sub-ms refolding reaction in 0.8 M urea in the presence of a 4-fold-higher concentration of ANS (4 mM) (blue circle) and a 2-fold-higher concentration of the protein (40 μM) (magenta square); and the observed fast rate constants monitored by Trp fluorescence (brown triangles), far-UV CD (green triangles), and FRET (teal triangles). In all cases, the errors bars indicating the spreads in the values, which were determined from two or more repetitions of the experiments, are smaller than the sizes of the symbols. (*c*) Arrhenius plot showing the temperature dependence of the apparent rate constant of the very fast phase. The slope of the plot yields an apparent activation energy of 0.6 kcal·mol^{-1}.

occurring in the absence of a dominant barrier (5, 7). Although non-Arrhenius kinetics could possibly also arise from the hydrophobic nature of the collapse reaction (36), this is unlikely because the activation enthalpy for the sub-ms folding reaction of cytochrome *c* was observed to be positive (35) when measured over a similar temperature range.

An examination of the results of earlier sub-ms kinetic measurements of the folding of several other proteins reveals that the observed rate constants of their sub-ms folding reactions also have no significant dependence on denaturant concentration (27, 35, 37–40). These folding reactions were assumed to be barrier-limited transitions principally because of the strong pragmatic belief that exponential kinetics can arise only from a barrier-limited process (40, 41). In this context, it should be noted that most ultrafast folding proteins (42, 43), which cross marginal free energy barriers, if any, during folding, have folding relaxation rates with denaturant dependences that are much weaker than expected from equilibrium experiments (7), and with temperature dependences that are also weak (7).

In a previous study of the sub-ms folding of barstar, the very fast folding reaction was assumed to be barrier-limited because its kinetics appeared sensitive to mutation. But the effects of the mutations were small: an assumed barrier was destabilized by $\leq$0.2 kcal·mol^{-1} by most mutations (27). The only mutations that appeared to have larger effects (larger φ values) were at residue positions located in helix 1, which is structured in the cold-denatured state from which folding was commenced (28). Not surprisingly, when folding is commenced from 8 M urea in which residual structure is absent, no structure appeared to be present in residues in I_E, which showed structure in the earlier temperature-jump study (33). Hence, it is likely that these mutations exert their effects by changing the stability of the unfolded state. On the other hand, the conclusion reached here that the initial folding reaction occurs not over a dominant free energy barrier but over many very low (less than or equal to k_BT) distributed barriers, which is based on the observation that the very fast folding rate constant cannot be perturbed by a change in denaturant concentration, is greatly strengthened by previous observations (see above), as well as the observed temperature dependence of its rate (Fig. 3*c*).

The slope of a plot of the log rate versus urea concentration is a measure of the change in solvent-accessible surface area (44). The observation that the very fast folding rate constant is independent of urea concentration suggests that any TS separating I_E from U would be identical, in terms of the solvent-accessible surface area, to U. In such a case, it is very unlikely that the TS and U would differ in free energy, and this would again imply that there is no significant barrier separating U from I_E. The complete lack of denaturant dependence also makes it unlikely that a mobile barrier separates U and I_E: such a barrier would move toward I_E with an increase in urea concentration due to a Hammond effect, and at least some denaturant-dependent decrease in the very fast rate would be expected.

In contrast to the kinetics of the very fast folding process, the kinetics of the fast (millisecond) folding reaction that follows appear to be barrier-limited, because the observed fast rate constant shows a significant dependence on the concentration of urea in which the folding reaction is carried out (Fig. 3*b*). The dependence of the rate of the ANS-fluorescence-monitored fast refolding phase on the concentration of urea is similar to that of the far-UV CD-monitored rate, as well as fluorescence- and FRET-monitored rates (Fig. 3*b*) (although the rates themselves appear to be probe-dependent), which suggests that these different probes report on the crossing of similar free energy barriers.

To confirm the principal result of this study, namely that the very fast sub-ms process does not involve the crossing of any substantial free energy barrier, it was first necessary to show that

the kinetics of the very fast phase are not (*i*) those of the bimolecular reaction of the binding of ANS to barstar; (*ii*) affected by the presence of ANS; and (*iii*) those of any transient protein aggregation reaction. This was done by showing that the very fast rate constant remained the same when a 4-fold-higher ANS concentration or a 2-fold-higher protein concentration was used (Fig. 3*b*).

Nature of the Initial Folding Transition. The initial very fast folding reaction produces significant specific secondary structure and hydrophobic clustering in I_E in strongly stabilizing but not in marginally stabilizing folding conditions (Fig. 1), but its observed rate constant does not depend on the extent of structure produced. For a folding reaction occurring in the absence of a significant free energy barrier, this is precisely what is expected. The initial folding reactions of proteins are expected to occur through multiple pathways so that kinetic bottlenecks are avoided (23, 45). It will be important to determine in future studies whether the pathway for the formation of I_E changes in different folding conditions and whether a dominant barrier is absent even in conditions where I_E is very strongly stabilized.

The observation that I_E forms gradually might imply that its helical secondary structure must also form gradually. Ultrafast temperature-jump studies on short peptides, which indirectly measure the rate of helix formation, suggest that helices form in the sub-microsecond to microsecond time domain (46–48), whereas a microsecond mixing experiment that measures helix formation more directly suggests that it occurs on the 150-μs time scale (49). Both types of measurements suggest that helix formation occurs in more than one step and might even occur by conformational diffusion (47). At present, it is not known whether secondary structure forms concurrently with chain contraction or with hydrophobic clustering, at least as revealed by ANS binding. In the context of a protein, chain compaction may induce helix formation in a noncooperative manner (50).

The earlier millisecond FRET-monitored folding kinetic experiments had indicated that the degree of chain contraction in I_E decreases with an increase in the urea concentration in which the folding is carried out (8, 9). I_E is therefore collapsed to different extents at different urea concentrations. Nevertheless, it is formed at the same very fast rate constant at these urea concentrations. The observation here that the rate constant of the formation of I_E is independent of the extent to which I_E is collapsed could be interpreted to signify the absence of a significant conformational entropy barrier, but it is more likely to be the consequence of small changes in chain and solvent entropy being continuously compensated for by weak enthalpic interactions as the collapse reaction proceeds over a multidimensional, rough energy surface (51).

Speed of the Initial Folding Reaction. The initial folding reaction of barstar has a time constant of ≈200 μs (Fig. 2) but does not appear to be slowed down by a dominant free energy barrier. What, then, slows it down? One possibility is that it is slowed down by the roughness of the energy surface (5, 43, 51): the folding protein molecules have to diffusively traverse a large multitude of local energy minima (conformational substates). This possibility is indeed suggested by the earlier observation that different regions of the polypeptide chain contract in an asynchronous manner in the initial folding reaction (9). Single-molecule studies have indicated that such gradual diffusive motion may occur over milliseconds (52) or even longer (53). In this context, it should be noted that the time scale of folding of other proteins reported to fold or unfold in a downhill manner appears to be in a similar (5–500 μs) time domain at ≈25°C (3, 7, 16, 17). In future studies it will be important to obtain a quantitative understanding of the free energy landscape sculpting that results in slow gradual folding or unfolding reactions.

In completely unfolded proteins at high denaturant concentration, diffusive interconversion of different conformations have been shown to occur on the ≈1- to ≈200-μs time scale (54, 55). The ≈1-μs motions, which scale as $n^{-3/2}$, represent the time scale for the diffusive formation of a single long-range contact between distal regions of the protein chain separated by n residues (56). Many hundreds of such contacts may form during a folding reaction. As expected, such diffusive fluctuations are slower in a more compact conformation than they are in U (52, 55). The slow (20–200 μs) fluctuations are thought to represent concerted chain motions, and it might be that such slow diffusive chain motions lead to the formation of I_E on an ≈200-μs time scale. If there are many small diffusive steps, each involving a very small barrier, and if protein folding is slowed down because the diffusive steps are slaved to solvent motions (57), then slower folders presumably just take many more diffusive steps to fold.

In this context it is important to ask why some very small proteins can fold completely within a few microseconds (7, 42, 43). Such ultrafast folding proteins have structures with low relative contact order, on which their microsecond folding rates depend (45). Their structures are predominantly local, helical in most cases; because more folding routes are likely to be available for local structures to form, especially for helices that can be nucleated at many locations in the sequence, folding can be ultrafast. In contrast, for more complex and larger proteins such as the α/β barstar, fewer folding routes are likely to be available for the initial folding reaction, which would slow down folding (45). Such proteins, which fold more slowly through a collapsed early intermediate populated at ≈1 ms, appear to possess more nonlocal contact clusters. The rate of formation of the early intermediate does not appear to depend on the relative contact order but instead appears to depend on the chain length as well as on the number of nonlocal contact clusters in the native protein (58). The formation of nonlocal contact clusters would naturally require many more diffusive steps, and, hence, the initial folding reactions of proteins such as barstar are slower.

Methods

Protein Expression and Purification. The single-Trp, single-Cys-containing mutant variants of barstar, Cys40 and Cys82, were produced as described earlier (8).

Continuous-Flow Microsecond Mixer. The two solutions to be mixed were pumped through a stainless steel mixer (*SI Methods* and Fig. S1) by using two low back-pressure HPLC pumps (Chromtech). An external gradient controller allowed simultaneous adjustment of the flow rates from the two pumps to give the desired mixing ratio. A quartz flow-through microcuvette (Hellma) with a 2-cm × 250-μm × 250-μm flow channel was used to monitor the progress of the reaction after mixing the reaction components in the mixer. The sample in the microcuvette was excited by the light output from a xenon arc lamp coupled to a monochromator. The entire 2-cm length of the cuvette was illuminated by focusing the light by using a cylindrical lens of 25-mm focal length. The emitted light was collected by using a liquid nitrogen-cooled, UV-coated, 2,048 × 512-pixel CCD camera (Jobin Yvon). An optical filter of suitable bandwidth was placed before the CCD chip to select the desired emission wavelength.

Equilibrium Unfolding Experiments. All of the fluorescence-monitored equilibrium data were acquired on a Fluoromax-3 spectrofluorimeter or on a Biologic SFM-4 stopped flow module, as described previously (8). All of the equilibrium and kinetic experiments were performed at 25°C.

Fast Kinetic Refolding Experiments. Far-UV CD and fluorescence measurements in the millisecond time domain were done by using a Biologic SFM-4 module, as described previously (8, 9, 26).

Ultrafast Kinetic Refolding Experiments. For the kinetic experiments in the sub-ms time domain, the solutions to be mixed were pumped at a total flow rate of 1 ml/s. The composition of the native buffer was altered so as to achieve

the desired final concentration of urea after a 1/10 dilution in the mixer. Data analysis is described in *SI Methods*.

ACKNOWLEDGMENTS. We thank B. Bagchi, M. K. Mathew, R. Varadarajan, and members of our laboratory for discussions. K.K.S. is the recipient of a Senior Research Fellowship from the Council of Scientific and Industrial Research, India. J.B.U. is the recipient of a J.C. Bose National Research Fellowship from the Government of India. This work was funded by the Tata Institute of Fundamental Research and by the Department of Biotechnology, Government of India.

1. Kubelka J, Hofrichter J, Eaton WA (2004) The protein folding speed limit. *Curr Opin Struct Biol* 14:76–88.
2. Munoz V (2007) Conformational dynamics and ensembles in protein folding. *Annu Rev Biophys Biomol Struct* 36:395–412.
3. Gruebele M (2005) Downhill protein folding: Evolution meets physics. *C R Biol* 328:701–712.
4. Karplus M (2000) Aspects of protein reaction dynamics: Deviations from simple behavior. *J Phys Chem B* 104:11–27.
5. Bryngelson JD, Onuchic JN, Socci ND, Wolynes PG (1995) Funnels, pathways, and the energy landscape of protein folding: A synthesis. *Proteins* 21:167–195.
6. Huang F, Sato S, Sharpe TD, Ying L, Fersht AR (2007) Distinguishing between cooperative and downhill protein folding. *Proc Natl Acad Sci USA* 104:123–127.
7. Naganathan AN, Doshi U, Munoz V (2007) Protein folding kinetics: Barrier effects in chemical and thermal denaturation experiments. *J Am Chem Soc* 129:5673–5682.
8. Sinha KK, Udgaonkar JB (2005) Dependence of the size of the initially collapsed form during the refolding of barstar on denaturant concentration: Evidence for a continuous transition. *J Mol Biol* 353:704–718.
9. Sinha KK, Udgaonkar JB (2007) Dissecting the non-specific and specific components of the initial folding reaction of barstar by multi-site FRET measurements. *J Mol Biol* 370:385–405.
10. Sherman E, Haran G (2006) Coil-globule transition in the denatured state of a small protein. *Proc Natl Acad Sci USA* 103:11539–11543.
11. Merchant KA, Best RB, Louis JM, Gopich IV, Eaton WA (2007) Characterizing the unfolded states of proteins using single-molecule FRET spectroscopy and molecular simulations. *Proc Natl Acad Sci USA* 104:1528–1533.
12. Lakshmikanth GS, Sridevi K, Krishnamoorthy G, Udgaonkar JB (2001) Structure is lost incrementally during the unfolding of barstar. *Nat Struct Biol* 8:799–804.
13. Li H, Frieden C (2007) Comparison of C40/82A and P27A C40/82A barstar mutants using ^{19}F NMR. *Biochemistry* 46:4337–4347.
14. Sadqi M, Fushman D, Munoz V (2006) Atom by atom analysis of global downhill protein folding. *Nature* 442:317–321.
15. Ahmed Z, Beta IA, Mikhonin AV, Asher SA (2005) UV-resonance Raman thermal unfolding study of Trp-cage shows that it is not a simple two-state miniprotein. *J Am Chem Soc* 127:10943–10950.
16. Sabelko J, Ervin J, Gruebele M (1999) Observation of strange kinetics in protein folding. *Proc Natl Acad Sci USA* 96:6031–6036.
17. Leeson DT, Gai F, Rodriguez HM, Greogoret LM, Dyer RB (2000) Protein folding and unfolding on a complex energy landscape. *Proc Natl Acad Sci USA* 97:2527–2532.
18. Zwanzig R (1988) Diffusion in a rough potential. *Proc Natl Acad Sci USA* 85:2029–2030.
19. Knott M, Chan HS (2006) Criteria for downhill protein folding: Calorimetry, chevron plot, kinetic relaxation and single molecule radius of gyration in chain models with subdued degrees of cooperativity. *Proteins* 65:373–391.
20. Hagen SJ (2007) Probe-dependent and non-exponential relaxation kinetics: Unreliable signatures of downhill protein folding. *Proteins* 68:205–217.
21. Gruebele M (2007) Comment on probe-dependent and non-exponential relaxation kinetics: Unreliable signatures of downhill protein folding. *Proteins* 70:1099–1102.
22. Saigo S, Shibayama N (2003) Highly non-exponential kinetics in the early phase refolding of proteins at low temperatures. *Biochemistry* 42:9669–9676.
23. Ellison PA, Cavagnero S (2006) Role of unfolded state heterogeneity and en-route ruggedness in protein folding kinetics. *Protein Sci* 15:564–582.
24. Shastry MC, Udgaonkar JB (1995) The folding mechanism of barstar: Evidence for multiple pathways and multiple intermediates. *J Mol Biol* 247:1013–1027.
25. Pradeep L, Udgaonkar JB (2002) Differential salt-induced stabilization of structure in the initial folding intermediate ensemble of barstar. *J Mol Biol* 324:331–347.
26. Pradeep L, Udgaonkar JB (2004) Osmolytes induce structure in an early intermediate on the folding pathway of barstar. *J Biol Chem* 279:40303–40313.
27. Nolting B, Golbik R, Fersht AR (1995) Submillisecond events in protein folding. *Proc Natl Acad Sci USA* 92:10668–10672.
28. Nolting B, Golbik R, Neira JL, Soler-Gonzalez AS, Fersht AR (1997) The folding pathway of a protein at high resolution from microseconds to seconds. *Proc Natl Acad Sci USA* 94:826–830.
29. Sridevi K, Lakshmikanth GS, Krishnamoorthy G, Udgaonkar JB (2004) Increasing stability reduces conformational heterogeneity in a protein folding intermediate ensemble. *J Mol Biol* 337:699–711.
30. Agashe VR, Shastry MC, Udgaonkar JB (1995) Initial hydrophobic collapse in the folding of barstar. *Nature* 377:754–757.
31. Moglich A, Joder K, Kiefhaber T (2006) End-to-end distance distributions and intrachain diffusion constants in unfolded polypeptide chains indicate intramolecular hydrogen bond formation. *Proc Natl Acad Sci USA* 103:12394–12399.
32. Chen K, Liu Z, Kallenbach NR (2004) The polyproline II conformation in short alanine peptides is noncooperative. *Proc Natl Acad Sci USA* 101:15352–15357.
33. Jha SK, Udgaonkar JB (2007) Exploring the cooperativity of the fast folding reaction of a small protein using pulsed thiol labeling and mass spectrometry. *J Biol Chem* 282:37479–37491.
34. Cho SS, Weinkam P, Wolynes PG (2008) Origins of barriers and barrierless folding in BBL. *Proc Natl Acad Sci USA* 105:118–123.
35. Hagen SJ, Eaton WA (2000) Two-state expansion and collapse of a polypeptide. *J Mol Biol* 297:781–789.
36. Oliveberg M, Tan YJ, Fersht AR (1995) Negative activation enthalpy in the kinetics of protein folding. *Proc Natl Acad Sci USA* 92:8926–8929.
37. Shastry MC, Roder H (1998) Evidence for barrier-limited protein folding kinetics on the microsecond time scale. *Nat Struct Biol* 5:385–392.
38. Teilum K, Maki K, Kragelund BB, Poulsen FM, Roder H (2002) Early kinetic intermediate in the folding of acyl-CoA binding protein detected by fluorescence labeling and ultrarapid mixing. *Proc Natl Acad Sci USA* 99:9807–9812.
39. Park SH, Shastry MC, Roder H (1999) Folding dynamics of the B1 domain of protein G explored by ultrarapid mixing. *Nat Struct Biol* 6:943–947.
40. Cellmer T, Henry ER, Kubelka J, Hofrichter J, Eaton WA (2007) Relaxation rate for an ultrafast folding protein is independent of chemical denaturant concentration. *J Am Chem Soc* 129:14564–14565.
41. Roder H, Maki K, Cheng H (2006) Early events in protein folding explored by rapid mixing methods. *Chem Rev* 106:1836–1861.
42. Yang WY, Gruebele M (2003) Folding at the speed limit. *Nature* 423:193–197.
43. Dyer RB (2007) Ultrafast and downhill protein folding. *Curr Opin Struct Biol* 17:38–47.
44. Schellman JA (1978) Solvent denaturation. *Biopolymers* 17:1305–1322.
45. Ghosh K, Ozkan SB, Dill KA (2007) The ultimate speed limit to protein folding is conformational searching. *J Am Chem Soc* 129:11920–11927.
46. Eaton WA, *et al.* (2000) Fast kinetics and mechanisms in protein folding. *Annu Rev Biophys Biomol Struct* 29:327–359.
47. Huang CY, *et al.* (2002) Helix formation via conformation diffusion search. *Proc Natl Acad Sci USA* 99:2788–2793.
48. Milkhonon AV, Asher SA, Bykov SV, Murza A (2007) UV Raman spatially resolved melting dynamics of isotopically labeled polyalanyl peptide: Slow α-helix melting follows 310-helices and π-bulges premelting. *J Phys Chem B* 111:3280–3292.
49. Kimura T, *et al.* (2002) Direct observation of the multistep helix formation of poly-L-glutamic acids. *J Am Chem Soc* 124:11596–11597.
50. Chan HS, Dill KA (1990) Origins of structure in globular proteins. *Proc Natl Acad Sci USA* 87:6388–6392.
51. Chavez LL, Onuchic JN, Clementi C (2004) Quantifying the roughness on the free energy landscape: Entropic bottlenecks and protein folding rates. *J Am Chem Soc* 126:8426–8432.
52. Baldini G, Cannone F, Chirico G (2005) Pre-unfolding resonant oscillations of single green fluorescent protein molecules. *Science* 309:1096–1100.
53. Rhoades E, Gussakovsky E, Haran G (2003) Watching proteins fold one molecule at a time. *Proc Natl Acad Sci USA* 100:3197–3202.
54. Chattopadhyay K, Elson EL, Frieden C (2005) The kinetics of conformational fluctuations in an unfolded protein measured by fluorescence methods. *Proc Natl Acad Sci USA* 102:2385–2389.
55. Chen H, Rhoades E, Butler JS, Loh SN, Webb WW (2007) Dynamics of equilibrium structural fluctuations of apomyoglobin measured by fluorescence correlation spectroscopy. *Proc Natl Acad Sci USA* 104:10459–10464.
56. Hagen SJ, Carswell CW, Sjolander EM (2001) Rate of intrachain contact formation in an unfolded protein: Temperature and denaturant effects. *J Mol Biol* 305:1161–1171.
57. Frauenfelder H, Fenimore PW, Chen G, McMahon BH (2006) Protein folding is slaved to solvent motions. *Proc Natl Acad Sci USA* 103:15469–15472.
58. Kamagata K, Kuwajima K (2006) Surprisingly high correlation between early and late stages in non-two-state protein folding. *J Mol Biol* 357:1647–1654.